

Effects of polarization-field tuning in GaInN light-emitting diodes

Jiuru Xu,¹ Martin F. Schubert,^{1,a)} Di Zhu,^{1,b)} Jaehee Cho,¹ E. Fred Schubert,¹ Hyunwook Shim,² and Cheolsoo Sone²

¹Future Chips Constellation, Department of Physics, Applied Physics, and Astronomy, and Department of Electrical, Computer, and Systems Engineering, Rensselaer Polytechnic Institute, Troy, New York 12180, USA

²R&D Institute, Samsung LED, Suwon 443-744, Korea

(Received 5 May 2011; accepted 21 June 2011; published online 26 July 2011)

III-V nitrides form the backbone of light-emitting diode (LED) technology. However, the relevance of the very strong polarization fields in III-V nitride LEDs remains unclear. Here, we demonstrate the tuning of polarization fields by mechanical force. For compressive strain in a GaInN LED epitaxial layer, we find: (i) redistribution of intensity within the electroluminescence spectrum; (ii) a decrease in the peak efficiency at low current densities; and (iii) an increase in light-output power at high current densities. These findings show the relevance of transport effects in the efficiency droop. © 2011 American Institute of Physics. [doi:10.1063/1.3609783]

III-V nitrides have been the subject of extensive studies, motivated by the role of GaInN light-emitting diodes (LEDs) as key building blocks in future lighting systems. Although much progress has been made, a significant challenge remains: Devices suffer from the efficiency droop—the well-known decrease of efficiency at high injection currents. The physical origin of efficiency droop remains attributed to a series of different physical phenomena.^{1–10}

Among common semiconductor material systems, a distinguishing feature of III-V nitride semiconductors is that they have very high spontaneous and piezo-electric polarization charges; they result in electric fields directed along the [0001] axis, the preferred growth axis.^{11–15} Sheet charges and associated electric fields strongly impact carrier transport and recombination dynamics in the active light-emitting region of GaInN LEDs.^{11–17}

Figure 1(a) illustrates the polarization-induced-sheet charges in the band diagram of a GaInN LED. In a typical active region, two types of sheet charges are of interest: (i) the charge at the interface between GaInN quantum wells (QWs) and GaN quantum barriers (QBs) of the multiple-quantum-well (MQW) active region and (ii) the charge at the interface between a GaN spacer layer and the AlGaIn electron-blocking-layer (EBL). Sheet charges (σ_A) at the QW/QB interfaces induce a strong electric field in the QW layers. As a result, the overlap of electron and hole wave functions is reduced, the radiative recombination rate is reduced, and the emission spectrum is red-shifted.¹⁶ Collectively, these effects are known as the quantum-confined Stark effect (QCSE).¹⁶ Furthermore, it has been recently shown that the capture of electrons into a QW having a strong electric field is reduced.¹⁷ In GaInN LEDs, it was found that the carrier distribution and recombination does not occur uniformly across all QWs, but concentrate at the last QW close to p-side of the device.^{18–20} As illustrated in Fig. 1(a), the positive sheet charge (σ_B) at the spacer/EBL hetero-interface attracts and accumulates electrons at the interface and, as a consequence, reduces the effective barrier height of the EBL.

^{a)}Present address: Micron Technology Inc., Boise, Idaho 83707.

^{b)}Author to whom correspondence should be addressed. Electronic mail: zhud3@rpi.edu.

The polarization fields in III-V nitrides have two components: The spontaneous and piezoelectric polarization fields; the former is determined by material composition and the latter is by strain.^{11,13} In this study, we alter the polarization fields in GaInN LEDs by externally straining the LED epilayers, and we measure the impact on the emission characteristics of the LED. The external strain on the LED epilayers is induced by mechanically changing the curvature of the LED-on-sapphire wafer, as illustrated in Fig. 1(b). Since the

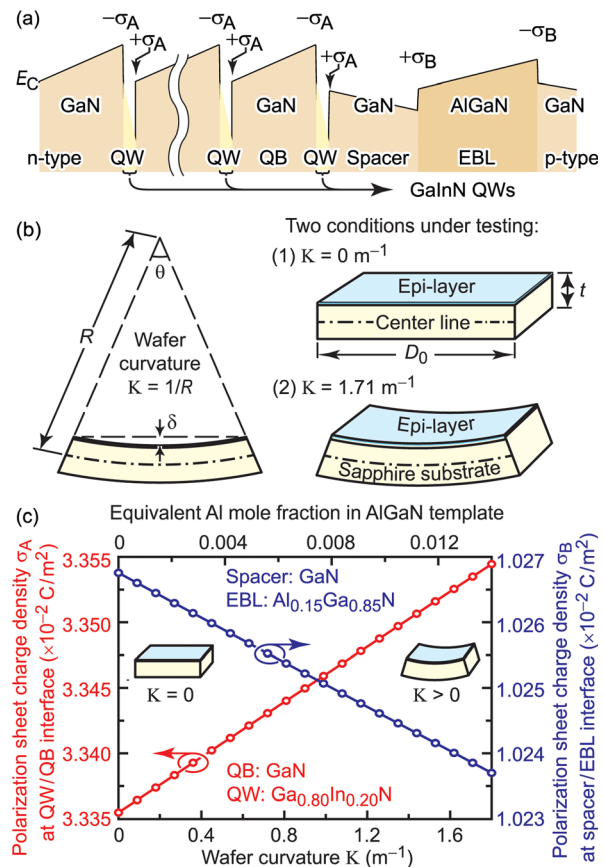


FIG. 1. (Color online) (a) Illustration of polarization sheet charges in conduction band diagram of GaInN LEDs, (b) illustration of an externally strained LED wafer, and (c) calculated polarization sheet charge as a function of an LED-on-sapphire wafer curvature including the equivalent aluminum fraction in a AlGaIn growth template.

sapphire substrate is much thicker than the LED epi-layers, the center line (neutral axis) of the sapphire wafer is assumed not to change with varying external strain. The arrangement results in LED epi-layers with additional compressive strain. The externally applied strain on the LED epi-layers alters the piezoelectric component of the polarization field and the polarization sheet charges at hetero-interfaces of the LED. Figure 1(c) shows the impact of wafer bending on the sheet charges σ_A in the MQW active region and the sheet charge σ_B in the spacer-EBL region. The sheet charges at the QW/QB hetero-interfaces (σ_A) increase with the wafer curvature. However, the sheet charges at the spacer/EBL hetero-interface (σ_B) decrease with the wafer curvature. The compressive strain could also be exerted by adding aluminum to a relaxed GaN growth template, as shown by the upper abscissa in Fig. 1(c). We note that the polarization sheet charges in the MQW active region and in the spacer-EBL region have two distinct trends as the wafer curvature increases. This provides us the opportunity to not only study the overall impact on the device performance of GaInN LEDs due to the polarization fields but also allows us to further identify the impact of a polarization field in a specific region of GaInN LEDs.

The LED epitaxial structures are grown on (0001) sapphire substrates by metal-organic-chemical-vapor deposition. A five-period MQW active region is grown, consisting of 3-nm-thick $\text{Ga}_{0.8}\text{In}_{0.2}\text{N}$ QWs and 12-nm-thick GaN QBs. The center wavelength of electroluminescence (EL) is around 445 nm. Wafers are processed into lateral LED structures $1 \times 1 \text{ mm}^2$ in area and left unencapsulated in wafer form. The devices are state-of-the-art with absolute internal quantum efficiencies greater than 50%. The LED-on-sapphire wafer is bent by external mechanical force. Figure 2 shows a front-view photograph enhanced by illustration of major components. The wafer is positioned on a glass slide. The two ends of the glass slides are on top of rigid sample holders. A curved anvil, using DuPont Company Delrin material, was fabricated. The anvil is pressing downwards at the center of the sample. The bending displacement is measured by a digital dial underneath the glass slide. Uni-axial curvature is achieved on the LED-on-sapphire wafer. The wafer curvature achieved is limited by the wafer's ability to be deformed elastically. The curvature of the sample is calculated from the following quantities: The bending displacement, the distance between the two rigid sample holders, and the substrate thickness. EL characteristics are measured on the same LED chip with all other conditions fixed except the

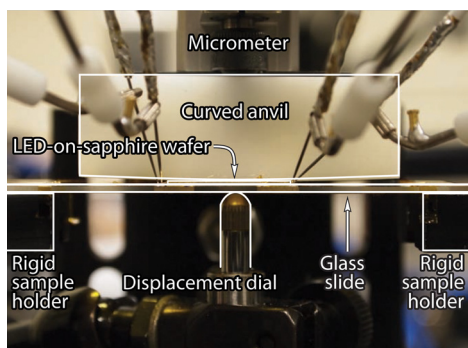


FIG. 2. (Color online) Front view of the LED-on-sapphire wafer bending setup with illustrations of all major components.

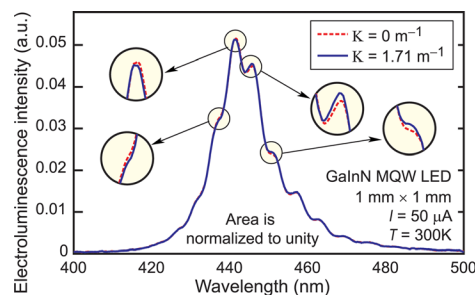


FIG. 3. (Color online) Electroluminescence spectra comparison of the same GaInN LED at two wafer curvatures, with “zoomed-in” views at the spectral sub-peaks.

wafer curvature, which is either zero or 1.71 m^{-1} . The wafer bowing after epitaxy is usually about 0.1 m^{-1} , much smaller than the induced curvature, and therefore negligible.

Next, we present EL spectra and efficiencies of the same GaInN LED measured under two conditions: (i) when the wafer is relaxed and (ii) when the wafer is externally strained to the curvature of 1.71 m^{-1} . Figure 3 shows the EL spectra comparison at $50 \mu\text{A}$ DC forward current between wafer curvatures of $K = 0 \text{ m}^{-1}$ and $K = 1.71 \text{ m}^{-1}$ with magnified views at the etalon-induced sub-peaks of the emission spectra. A low forward current is chosen to minimize the free-carrier-screening effect of the electric field inside the QWs, so that the change of the polarization field is more profound. The changes shown in Fig. 3 are described as follows: while the sub-peaks below the center wavelength exhibit an increase in intensity, the sub-peaks above the center wavelength exhibit a decrease in intensity. These distinct changes in intensity represent a red-shift of the EL spectrum with a wafer curvature of $K = 1.71 \text{ m}^{-1}$ compared to the EL spectrum at $K = 0 \text{ m}^{-1}$. The red-shift is verified by calculation of the centroid wavelength, which shifts from 445.84 nm to 445.88 nm as the wafer curvature increases from $K = 0 \text{ m}^{-1}$ to $K = 1.71 \text{ m}^{-1}$. Although the differences in emission characteristics are small, the changes are specific, significant, and highly reproducible.

In the MQW active region, the increase of the sheet charges σ_A increases the electric field inside the QWs and consequently increases the QCSE. The emission spectrum is expected to shift towards longer wavelength and the associated low-current efficiency is expected to decrease. QCSE is more severe at low injection current densities, since the free carriers have screening effects on the electric field in the QW layers. The measured spectral red-shift confirms that the tuning of polarization field in the GaInN LED is accomplished by the wafer-bending method and its trend is consistent with the calculation shown in Fig. 1(c). The red-shift is consistent with the increase in electric field in the MQW region caused by the stronger curvature.

Figure 4(a) shows the measured EL efficiency as a function of current density on the same GaInN MQW LED for wafer curvatures of $K = 0 \text{ m}^{-1}$ and $K = 1.71 \text{ m}^{-1}$ with magnified views of both the efficiency-peak region (at low current densities) and the efficiency-droop region (at high current densities). There are two distinct results obtained from the measurements: first, in the efficiency-peak region at the low current densities, the efficiency of the GaInN LED with induced wafer curvature is lower than that of the same LED without induced curvature. Second, in the efficiency-

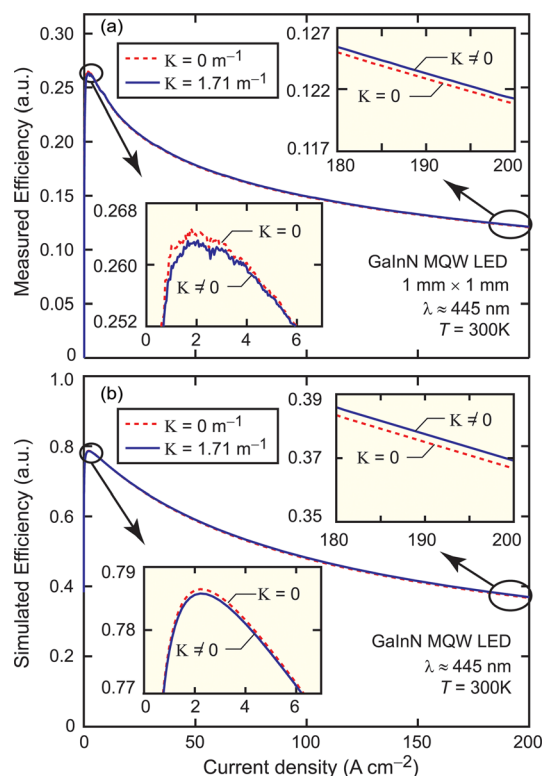


FIG. 4. (Color online) (a) Measured efficiency comparison of the same GaInN LED at two wafer curvatures, with “zoomed-in” views at the efficiency-peak region at low currents and the efficiency droop region at high currents and (b) LEDSIM-simulated efficiency comparison with the same conditions as in (a).

droop region at high current densities, the efficiency of the GaInN LED with induced wafer curvature is higher than that without induced curvature. As a result, there is a cross-over of the two efficiency curves and the LED wafer with induced curvature has a lower efficiency droop. These experimental results can be explained as follows: the lower efficiency measured at low current densities is consistent with the increase in QW electric field and associated QCSE. The efficiency increase at high current densities is consistent with a reduction of the positive sheet charge at the spacer-EBL interface, which mitigates electron leakage out of the active region. The mitigation effect on electron-leakage is more obvious at high injection current densities, since the electron leakage increases with carrier concentration.

Along with the measured efficiency under different strain conditions, device simulations are performed on the same GaInN LED using the LEDSIM simulation tool. The simulation results are shown in Fig. 4(b) which has the same efficiency comparison to the experimental results in Fig. 4(a). The simulated and the measured efficiency behaviors show excellent agreement in both the overall trend and the detailed comparisons in the magnified views.

We note that the results presented here could not be readily explained if Auger recombination were to be the dominant cause of the droop. A larger QCSE (stronger field in QW) should enhance Auger recombination^{8,9} and thus increase droop. However, our experiments reveal a decrease in droop upon application of the external compressive force. We also note that the results presented here shed light on the use of GaInN underlayers located below the active region.^{21,22}

GaInN underlayers induce tensile strain in the MQW region thereby reducing the QCSE and increasing low-current efficiency (although without alleviating the droop problem).

In summary, we have tuned the polarization-field via external mechanical force and directly measured the effects on carrier recombination and transport in the same GaInN LED. With this design of experiment, we have excluded the sample-to-sample and wafer-to-wafer variation, which has not been achieved in previous studies of the polarization field. The tuning of the polarization field is experimentally confirmed by the red-shift of the emission spectrum at low current level, which is a well-known consequence of QCSE in GaInN LEDs. Tuning the polarization field reduces peak efficiency, enhances high current efficiency, and reduces efficiency droop in GaInN LEDs. Simulation and experiments show excellent agreement. Our results show that the polarization field has clear impact on carrier transport and recombination, and suggest that the electron leakage out of the active region plays an active role in the efficiency droop in GaInN-based LEDs.

The authors gratefully thank Samsung LED, the National Science Foundation, New York State, and Sandia National Laboratory’s Solid-State Lighting Science Center, an Energy Frontiers Research Center funded by the U.S. Department of Energy, Office of Science, and Office of Basic Energy Sciences.

- ¹M. F. Schubert, J. Xu, J. K. Kim, E. F. Schubert, M. H. Kim, S. Yoon, S. M. Lee, C. Sone, T. Sakong, and Y. Park, *Appl. Phys. Lett.* **93**, 041102 (2008).
- ²J. Xu, M. F. Schubert, A. N. Noemaun, D. Zhu, J. K. Kim, E. F. Schubert, M. H. Kim, H. J. Chung, S. Yoon, C. Sone, and Y. Park, *Appl. Phys. Lett.* **94**, 011113 (2009).
- ³M. H. Kim, M. F. Schubert, Q. Dai, J. K. Kim, E. F. Schubert, J. Piprek, and Y. Park, *Appl. Phys. Lett.* **91**, 183507 (2007).
- ⁴M. F. Schubert, S. Chhajed, J. K. Kim, E. F. Schubert, D. D. Koleske, M. H. Crawford, S. R. Lee, A. J. Fischer, G. Thaler, and M. A. Banas, *Appl. Phys. Lett.* **91**, 231114 (2007).
- ⁵I. A. Pope, P. M. Snowton, P. Blood, J. D. Thomson, M. J. Kappers, and C. J. Humphreys, *Appl. Phys. Lett.* **82**, 2755 (2003).
- ⁶J. Xie, X. Ni, Q. Fan, R. Shimada, U. Ozgur, and H. Morkoc, *Appl. Phys. Lett.* **93**, 121107 (2008).
- ⁷I. V. Rozhansky and D. A. Zakheim, *Phys. Status Solidi C* **3**, 2160 (2006).
- ⁸Y. C. Shen, G. O. Müller, S. Watanabe, N. F. Gardner, A. Munkholm, and M. R. Krames, *Appl. Phys. Lett.* **91**, 141101 (2007).
- ⁹N. F. Gardner, G. O. Müller, Y. C. Shen, G. Chen, S. Watanabe, W. Götz, and M. R. Krames, *Appl. Phys. Lett.* **91**, 243506 (2007).
- ¹⁰B. Monemar and E. B. Sernelius, *Appl. Phys. Lett.* **91**, 181103 (2007).
- ¹¹F. Bernardini, “Spontaneous and piezoelectric polarization: Basic theory vs. practical recipes,” in *Nitride Semiconductor Devices: Principles and Simulation*, edited by J. Piprek (WILEY-VCH Verlag GmbH & Co. KGaA, Weinheim, Germany, 2007).
- ¹²V. Fiorentini, F. Bernardini, and O. Ambacher, *Appl. Phys. Lett.* **80**, 1204 (2002).
- ¹³A. Zoroddu, F. Bernardini, P. Ruggerone, and V. Fiorentini, *Phys. Rev. B* **64**, 045208 (2001).
- ¹⁴F. Bernardini, V. Fiorentini, and D. Vanderbilt, *Phys. Rev. B* **63**, 193201 (2001).
- ¹⁵F. Bernardini and V. Fiorentini, *Phys. Status Solidi A* **90**(1), 65 (2002).
- ¹⁶T. Takeuchi, S. Sota, M. Katsuragawa, M. Komori, H. Takeuchi, H. Amano, and I. Akasaki, *Jpn. J. Appl. Phys.* **36**, L382 (1997).
- ¹⁷M. F. Schubert and E. F. Schubert, *Appl. Phys. Lett.* **96**, 131102 (2010).
- ¹⁸A. David, M. J. Grundmann, J. F. Kaeding, N. F. Gardner, T. G. Mihopoulos, and M. R. Krames, *Appl. Phys. Lett.* **92**, 053502 (2008).
- ¹⁹A. David and M. J. Grundmann, *Appl. Phys. Lett.* **96**, 103504 (2010).
- ²⁰D. Zhu, A. N. Noemaun, M. F. Schubert, J. Cho, E. F. Schubert, M. H. Crawford, and D. D. Koleske, *Appl. Phys. Lett.* **96**, 121110 (2010).
- ²¹T. Akasaka, H. Gotoh, T. Saito, and T. Makimoto, *Appl. Phys. Lett.* **85**, 3089 (2004).
- ²²P. C. Tsai, Y. K. Su, W. R. Chen, and C.-Y. Huang, *Jpn. J. Appl. Phys.* **49**, 04DG07 (2010).